Minimax Theory and its Applications

Volume 11 (2026), No. 2s, 754 to 769

Numerical Representation of Incompressible Casson Fluid Flow through A Darcian medium Along Solutal Transformation And Electro Magnetic Heat Emission on A Vertical Cone

R. Kirthika[1] , S. Karthikeyan[2]

[1,2]Department of Mathematics, Erode Arts and Science College, Erode-638009, Tamil Nadu, India
Email: rkirthikamaths@gmail.com, ORCID: 0009-0001-7664-6807; 0000-0002-6573-625X

Abstract
The subject investigates the influence of porous-medium resistance, reactivity of chemical substancesand radiative effects due to heat on steady axisymmetric flow within the boundary layer of an incompressible Casson fluid around a vertical cone.The present study considers a non-Newtonian fluid governed by the Casson fluid model. The fluid occupies the conical region confined by the conical surface and the horizontal disc, which may be maintained in either a rotating or stationary state considering thermal and mass transport.The model extends the existing formulation by incorporating the collective effects of a uniform magnetic field applied in the vertical direction, Ohmic dissipation, and chemical reaction.The governing relations for the Casson fluid are expressed in terms of coordinates. By considering suitable similarity transformations, the governing partial differential equations describing momentum, energy, and mass transport are reduced to a coupled system of nonlinear ordinary differential equations and it results to a set of coupled nonlinear ordinary equations concerning velocity, temperature, and nanoparticles concentration distributions.Using suitable similarity variables, the governing equations for momentum, energy, and mass transport are reduced to a coupled system of nonlinear ordinary differential equations. The resulting formulation characterizes the velocity, temperature, and nanoparticle concentration distributions.

The analytical results are represented through graphical and tabular representations. The purpose of this research is to examine the impact of cone and disc rotation and the influence of other governing parameters under two alternative rotational configurations. Also, the influence of the cone angle and disc is investigated as a result of its considerable application in a wide spectrum of engineering and industrial applications. The effects of the porous medium are represented through Darcy resistance, with thermal radiation accounted for using the Rosseland diffusion approximation. Furthermore, species transport is governed by molecular diffusion in a homogeneous environment a first-order reaction mechanism.From the results, the analysis shows that an increase in the rotation parameters results in a decrease in thefluid temperature and radial velocity, whereas the azimuthal velocity is enhanced.

System of equations was solved by RK method with boundary layer conditions.With increase in the chemical-reaction parameter, it reduces concentration inside the boundary layer for a destructive reaction. The mathematical formulation governing continuity, momentum, energy, and concentration is formulated under boundary-layer assumptions. Suitable nondimensional variables are introduced to obtain a coupled nonlinear system containing the Casson parameter, porosity parameter, radiation parameter, buoyancy ,Prandtl and Schmidt number

The Casson parameter significantly alters momentum diffusion because of the rheological charactertics of the fluid with yield-stress. It involves a mathematical structure on transport processes involving non-Newtonian fluids in porous geometries and is relevant to geothermal systems, catalytic reactors, polymer processing, biomedical transport and thermal engineering applications.

Keywords: Casson fluid; vertical cone; porous medium; thermal radiation; chemical reaction; boundary- layer conditions; numerical solution.

Introduction

Non-Newtonian fluid transport near curved surfaces[1] is relevant to many industrial and biological processes in which the constitutive relation between stress and strain rate is not adequately represented by Newtonian viscosity. Blood, printing inks, polymeric materials, drilling fluids and several food products[2] exhibit yield-stress or shear-dependent characteristics. ACasson model is a well-established rheological representation for materials with a finite yield stress.

Conical surfaces occur in heat-transfer equipment[3], aerospace components, thermal probes, chemical-processing devices and other engineering systems. When a fluid moves along or around a cone embedded in a porous matrix, the porous skeleton introduces an additional resistance to momentum transport. The resulting interaction[4] between viscous diffusion, buoyancy and Darcy resistance can substantially modify the velocity and thermal boundary layers.

Radiative heat transfer[5] becomes important at elevated temperatures, while chemical reaction can strongly influence species transport in catalytic, environmental and reactive systems. A combined model[6] involving Casson rheology, porous resistance, thermal radiation and first-order chemical reaction therefore provides a useful framework for coupled momentum, heat and mass transfer.

A study is focused specifically on the role of porosity, thermal radiative effects and reaction effects on Casson fluid flow around a vertical cone. A principal contribution[7] is a unified formulation in which the effects are represented by nondimensional parameters and investigated through the momentum, thermal, solutaldistributions with wall-transfer characteristics. The earlier source text[8][9] contained an additional, unrelated model for rotating cone-disc nanofluid flow with MHD, Brownian motion, thermophoresis, Ohmic dissipation and Homotopy perturbation analysis. Those passages have been excluded from this revision to maintain consistency with the stated problem.

Magnetohydrodynamics (MHD)[10] is utilized in fluid-mechanics models to describe the behavior of fluid with finite electrical conductivity in an imposed magnetic field.Magnetohydrodynamics deals with the coupled interaction between the motion of electrically conducting fluids and electromagnetic fields.[11] When an Magneto Hydro dynamics through an applied magnetic field, the interaction between the fluid motion and the imposed magnetic flux induces an electric current which current interacts with the magnetic flux, generating a Lorentz force that acts as a body force on the fluid.

Owing to its broad[12] physical significance, inherent complexity, and associated mathematical challenges, magnetohydrodynamics has attracted considerable research attention. The introduction of nanofluids[13] has further expanded the scope of MHD studies, leading to significant advances in the investigation of coupled momentum, heat, and mass transport phenomena.The governing flow equations [14] were reduced to a coupled system NL-ODE through the introduction of appropriate transformations.The present investigation[15] incorporates the influence of an imposed field of magnets on flow as such adopted by extensive relevance of magneto hydrodynamic (MHD) effects in practical engineering and industrial applications,.

[16]Owing to its rheological behaviour, it has been extensively investigated for various engineering applications [17]. It represents an important class of non-Newtonian fluids [18] and finds applications in several fields, including biomedical, polymer processing, and metal-forming processes.

Casson fluid represents a class of fluid exhibiting non Newtonian characteristics [19] between shear stress and velocity gradient is inherently nonlinear. [20]Due to its flow characteristics, the Casson fluid has attracted considerable attention in engineering and applied sciences. [21]This distinctive flow characteristics of Casson fluids make them suitable for applications in biomechanics, polymer processing, metallurgy, and a variety of industrial processes.

The Casson fluid model [22] gives an effective approach for analyzing the flow behaviour of fluids exhibiting non-zero plastic dynamic viscosity which is suitable for describing the rheological characteristics of blood.Furthermore, Casson-type fluid behavior is observed in several complex fluids and industrial materials including blood and other biological fluids, as well as products such as paints, synthetic lubricants, coal–water mixtures, tomato sauce, honey, soup and jelly.Optimizing thermal performance [23]of chemically reactive and thermally radiativenanofluid flow withconvective heating and tribo electric effect of nanoparticles was derived. [24]Influence of electromagnetic field on chemically reacting two phase second grade model over an inclined permeable surface in energy equation was explained.[25]Mass transfer of fluid in a permeable matrices was determined.[26]Under chemically reacting conditions and thermal radiations over stretching surface was

explained. [27]Combined effects of thermal radiation and mass diffusion on MHD fluid flowanalysed the governing equations. [28][29]Time dependence of Chemical reaction and heat transfer and the stream function was obtained.[30] Influence of Casson fluid flow past a vertically oriented cone subjected to higher order chemical reactions.[31][32] Solving the equations by numerical approach in Rungekutha and shooting methods.[33]Viscous dissipation effect on temperature and concentration.[34]The flow within the boundary layer region adjacent to the surface with widespread applications of MHD.[35][36] Numerical study on Non Newtonian fluid by solving the differential equations Rosseland approximation in first order taylor was determined.

Since nonlinear differential equations generally restrict closed-form analytical solutions, approximate and numerical techniques are widely used to obtain meaningful solutions. Conventional perturbation methods are often restricted to problems containing a suitably defined small parameter, which may not be available in many nonlinear systems. Consequently, identifying an appropriate perturbation parameter can itself be challenging require specialized analytical procedures.

Literature Review

Prior analyses of Casson boundary layers has a magnetic fields, slip, and chemical reactions on vertical cone. Studies on cone demonstrate geometric thickening of the boundary layer. Porous-media resistance has been shown to attenuate velocities, and radiative heat transfer to augment temperatures—yet their concurrent action with Casson rheology around vertical cone remains comparatively underexplored. The present work closes this gap by restricting attention to Casson fluids and isolating the roles of porosity and radiation. The present formulation addresses this combined transport setting than the cylindrical and stretching surfaces.

Physical Model and Assumptions

Consider steady, laminar and axisymmetric incompressible Casson fluid flow is consideraround a vertically oriented cone enclosedwithin a homogeneous isotropic porous medium. Let x denote the coordinate is measured in the direction along the cone surface from the vertex , whereasy the perpendicularto the cone surface. The associated velocity components are u and v. The wall thermal and solutal are denoted by $T_W$and C_W, while $T_\infty$and $C_\infty$are the ambient values. The porous matrix is modeled using Darcy resistance. A homogeneous first-order destructive chemical reaction acts on the transported species. Thermal radiative effects are incorporated through the Rosseland approximation.

The flow is treated as stationary, axisymmetric and non - turbulent.The fluid follows the Casson constitutive relation.The porous medium is homogeneous and isotropic and obeys Darcy resistance.The properties of the fluid are treated as constant except for density variations in the buoyancy terms.Buoyancy effects are incorporated using the Boussinesq approximation.Radiative heat transfer is modeled by the Rosseland diffusion approximation. The chemical reaction is homogeneous, first order and destructive.

Casson Fluid Model

The Casson model represents a yield-stress fluid. In the boundary-layer reduction used in the source manuscript, the influence of the rheology is represented by the Casson parameter β. The effective viscous contribution is written in the form$\nu\left(1+\frac{1}{\beta}\right)\frac{\partial^2 u}{\partial y^2}$(1)

Where as β represent a stronger yield-stress contribution even it tends to ∞.

System of Governing Equations

Continuity equation

For steady, incompressible boundary-layer flow, the continuity equation is

$$\frac{\partial u}{\partial x}+\frac{\partial v}{\partial y}=0 \quad (2)$$

Momentum equation

The momentum balance equation is given by

$$u\ \frac{\partial u}{\partial x} + v\ \frac{\partial v}{\partial y} = \ v\left(1+\frac{1}{\beta}\right)\frac{\partial^2 u}{\partial y^2} - \left(\frac{v}{K}\right)\ u + g\beta T(\ T - \ T_\infty) + g\beta C(\ C - \ C_\infty)(3)$$

Here, (ν) denotes the kinematic viscosity of the fluid ,(K) represents the permeability of the porous medium, A (g) denotes the acceleration due to gravity, and (βT) is thecoefficient of thermal expansion and (βC) is the concentration expansion coefficient. The term $-\left(\frac{v}{K}\right)$ urepresents Darcy resistance.

Energy equation

The energy equation is given by

$$u\ \frac{\partial T}{\partial x} + v\ \frac{\partial T}{\partial y} = \alpha\frac{\partial^2 T}{\partial y^2} - \left(\frac{1}{\rho cp}\right)\frac{\partial q_r}{\partial y}(4)$$

Radiative heat flux

The q_r equation is given by

$$q_r = \ -\frac{\left(\frac{4\sigma^*}{3k^*}\right)\partial(T^4)}{\partial y}\ (5)$$

Under the approx.., the fourth-power temperature term is linearized about the ambient temperature. This produces a radiation parameter in the nondimensional energy equation.

Concentration equation

The concentration equation is given by

$$u\frac{\partial C}{\partial x} + \ v\frac{\partial C}{\partial y} = \ D\frac{\partial^2 C}{\partial y^2} - \ k_r(C - C_\infty)(6)$$

Here D is the molecular Diffusion coefficient and $k_r$is the first-order reaction coefficient. A positive reaction parameter corresponds to a destructive reaction in the formulation adopted here.

Boundary Conditions

A prescribed boundary conditions are

$$u\ = 0\ ,\ \ v\ = 0\ ,\ \ \ T = \ T_W,\ \ C = \ C_W,\ \ (7)$$

Far from the cone, the flow and transport variables approach the ambient state:

$$T \rightarrow \ T_\infty,\ \ \ C \rightarrow \ C_\infty \ \ \text{as} \ \ \ y \rightarrow \infty \ \ \ (8)$$

Nondimensional Formulation by similarity reduction

Define the dimensionless temperature and concentration variables by

$$\theta\ = \frac{T - T_\infty}{T_w - T_\infty}, \varphi\ = \frac{C - C_\infty}{C_w - C_\infty}\ (9)$$

After introduction of the stream function and similarity coordinate, the normalized nonlinear ODEs and A similarity coordinate η and stream function ψ are selected according to the cone geometry and the chosen buoyancy scaling. With an appropriate choice, the continuity equation is satisfied identically. The source manuscript gives the following representative reduced system:

$$\left(1+\frac{1}{\beta}\right)f'' + a_1\ ff' - a_2(f')^2 - Da^{-1}f' + \lambda T_\theta + \ \lambda C_\varphi = 0(10)$$

$$(1 + R)\ \theta'' + a_3 Pr\ f\ \theta' \ = 0 \ \ \ (11)$$

$\varphi'' + a_4\,Sc\,f\,\varphi' - Sc\,\gamma\,\varphi = 0$ (12)

The coefficients $a_1 - a_4$ depend on the exact similarity scaling and cone geometry. Because the source manuscript does not provide those cone-specific coefficients in extractable form, they must be derived explicitly and checked from the dimensional model before a journal submission.

Equations (10)–(12) should therefore be regarded as the representative reduced system retained for the manuscript revision, not as an independently validated final cone solution.

Stream-function transformation

Introduce the stream function $\psi(x, y)$through

$$u = \frac{\partial\psi}{\partial y}, \qquad v = -\frac{\partial\psi}{\partial x}. \tag{13}$$

Differentiation gives

$$\frac{\partial u}{\partial x} = \psi_{xy}, \quad \frac{\partial v}{\partial y} = -\psi_{xy}. \tag{14}$$

Hence $\frac{\partial u}{\partial x} + \frac{\partial v}{\partial y} = 0$ identically

Similarity coordinate

Introduce a similarity coordinate and ψ scale in the general form

$$\eta = y\Lambda(x), \quad \psi = \Psi(x)f(\eta). \tag{15}$$

The derivative of η with respect to y is

$$\eta_y = \Lambda(x), \tag{16}$$

and with respect to x is

$$\eta_x = y\Lambda'(x). \tag{17}$$

Using $\psi = \Psi f(\eta)$, the tangential velocity becomes

$$u = \psi_y = \Psi(x)f'(\eta)\eta_y = \Psi\Lambda f'. \tag{18}$$

The normal velocity is

$$v = -\psi_x = -\Psi' f - \Psi f'\eta_x = -\Psi' f - \Psi y\Lambda' f'. \tag{19}$$

Transformation of the thermal field

Define the dimensionless temperature

$$\theta(\eta) = \frac{T - T_\infty}{T_W - T_\infty}. \tag{20}$$

Thus

$$T = T_\infty + (T_W - T_\infty)\theta(\eta). \tag{21}$$

Differential with respect to θ in terms of y

$$T_y = (Tw - T\infty)\theta'\eta_y = (Tw - T\infty)\Lambda\,\theta'. \tag{22}$$

Differential with respect to θ in terms of y

$$T_{yy} = (Tw - T\infty)\Lambda^2\theta''. \tag{23}$$

Differential with respect to θ in terms of x

$$T_x = (Tw - T\infty)\theta'\eta_x. \quad (24)$$

Rosseland radiation reduction

The Rosseland approximation gives $q_r = -\frac{\left(\frac{4\sigma^*}{3k^*}\right)\partial(T^4)}{\partial y}$

For moderate temperature differences, expand T^4 about T_∞ using a first-order Taylor approximation:

$$T^4 = T_\infty^4 + 4T_\infty^3 (T - T_\infty) + O((T - T_\infty)^2). \quad (25)$$

Omitting the higher terms,

$$\frac{\partial(T^4)}{\partial y} \approx \frac{4T_\infty^3 \partial T}{\partial y}. \quad (26)$$

Therefore

$$q_r \approx -\left(16\sigma^* \frac{T_\infty^3}{3k^*}\right) T_y \quad (27)$$

and

$$\frac{\partial q_r}{\partial y} \approx -\left(16\sigma^* \frac{T_\infty^3}{3k^*}\right) T_{yy} \quad (28)$$

Substitution into the energy equation gives an effective thermal diffusion term:

$$uT_x + vT_y = \left[\alpha + 16\sigma^* \frac{T_\infty^3}{3\rho c_{pk^*}}\right] T_{yy} \quad (29)$$

After division by α and nondimensionalization, the radiative contribution is represented by the factor (1+R) in the normalized energy equation.

Transformation of the concentration field

Define $\varphi(\eta)$

Hence

$$C = C_\infty + (C_W - C_\infty)\varphi(\eta), \quad (30)$$

$$C_y = (C_W - C_\infty)\Lambda\varphi', \quad (31)$$

$$C_{yy} = (C_W - C_\infty)\Lambda^2\varphi''. \quad (32)$$

The chemical reaction term transforms as

$$-k_r(C - C_\infty) = -k_r(C_W - C_\infty)\varphi. \quad (33)$$

Transformation of the momentum equation

From . $u = \psi_y = \Psi(x)f'(\eta)\eta_y = \Psi\Lambda f'$. (34)

$u = \Psi\Lambda f'$.

Differentiation of (34) gives

$$u_x = (\Psi\Lambda)'f' + \Psi\Lambda f''\eta_x. \quad (35)$$

Differentiation of (34) gives

$$u_y = \Psi\Lambda^2 f'', \quad (36)$$

$$u_{yy} = \Psi\Lambda^3 f'''. \quad (37)$$

Therefore the convective terms are

$$uu_x = \Psi\Lambda f'[(\Psi\Lambda)' f' + \Psi\Lambda f'' \eta_x], \quad (38)$$

$$vu_y = [-\Psi' f - \Psi\eta_x' f]\Psi\Lambda^2 f''. \quad (39)$$

Combining above terms containing η_x cancel according to the stream-function construction, leaving the standard similarity combination of ff″ and (f′)² after division by the common x-dependent scale. The Casson diffusion term is

$$\nu\left(1+\frac{1}{\beta}\right)u_{yy} = \nu\left(1+\frac{1}{\beta}\right)\Psi\Lambda^3 f'''. \quad (40)$$

The Darcy resistance term is

$$-\left(\frac{\nu}{K}\right)u = -\left(\frac{\nu}{K}\right)\Psi\Lambda f'. \quad (41)$$

The thermal and concentration buoyancy contributions become proportional to θ and φ, respectively. After introduction of the characteristic length L and Darcy number $Da = \frac{K}{L^2}$, the normalized momentum equation adopted for the numerical study is

$$\left(1+\frac{1}{\beta}\right)f''' + ff'' - (f')^2 - Da^{-1}f' + \lambda T_\theta + \lambda C_\varphi = 0. \quad (42)$$

Reduction of the energy equation,Concentration equation and boundary conditions

The dimensional energy equation becomes, after cancellation of the temperature scale and division by the common similarity factor,

$$(1+R)\theta'' + Pr\, f\theta' = 0, \quad (43)$$

where

$$Pr = \frac{\nu}{\alpha}.$$

The dimensional species equation becomes, after nondimensionalization,

$$\varphi'' + Sc\, f\, \varphi' - Sc\, \gamma\, \varphi = 0, \quad (44)$$

with

$$Sc = \frac{\nu}{D}, \qquad \gamma = \frac{k_r^2 L}{\nu}.$$

The term −Scγφ represents the removal of species by a destructive first-order reaction.

The relevant boundary conditions are

$$f(0) = 0\ , f'(0) = 0, \theta(0) = 1, \varphi(0) = 1; \quad f'(\eta_\infty) = 0, \theta((\eta_\infty) = 0, \varphi((\eta_\infty) = 0 \quad (45)$$

Numerical Solution Procedure: Runge–Kutta Shooting Method

The coupled nonlinear boundary-value problem is solved using the classical fourth-order Runge–Kutta (RK4) method combined with a shooting procedure. The approach to maintain the required accuracy during numerical integration. At each step, two solutions of different orders are calculated and their difference is used to estimate the numerical error unknown wall derivatives f″(0), θ′(0) and φ′(0) are treated as shootingparameters.Select$\beta, Da, R, Pr, Sc, \gamma, \lambda_T and\ \lambda_C and\ specify\ \eta_{max}$the RK4 step size h.

Introduce $y_1 = f, y_2 = f', y_3 = f'', y_4 = \theta, y_5 = \theta', y_6 = \varphi \; and \; y_7 = \varphi'$.

The seven first-order equations from $\eta = 0 \; to \; \eta = \eta_{max}$using classical RK4.

Form the terminal residuals $f'(\eta_{max}), \theta(\eta_{max}) and \; \varphi(\eta_{max})$ to the shooting parameters iteratively until the residual norm is below the prescribed tolerance.Repeat with smaller h and larger η_{max} confirm numerical convergence. Evaluating the wall shear measures from the converged wall gradients by Matlab RK4 and Shooting Implementation.For the classical fourth-order Runge–Kuttaprovided that the solution is sufficiently smooth

First-order system

The governing similarity equations derived from boundary-layer approximations were solved

$y_1 = f, y_2 = f', y_3 = f'', y_4 = \theta, y_5 = \theta', y_6 = \varphi, y_7 = \varphi'$.

$$y_1' = y_2, \quad y_2' = y_3,$$

$$y_3' = -\left(\frac{y_1 y_3 - y_2^2 - y_2}{Da}\right) + \left(\frac{\lambda_T y_4 + \lambda_C y_6}{1 + \frac{1}{\beta}}\right),$$

$$y_4' = \; y_5, \quad y_5' = -\frac{Pr \; y_1 y_5}{(1+R)},$$

$$y_6' = \; y_7, \quad y_7' = -Sc \quad y_1 y_7 + Sc \; \gamma y_6.$$

Iteration of Shooting techniques:

The unknown initial slopes $s_1 = f''(0), s_2 = \theta'(0) \; and \; s_3 = \varphi'(0)$ are iteratively corrected.

The terminal residual vector is $E = [f'(\eta_\infty), \theta(\eta_\infty), \varphi(\eta_\infty)]^T$ and the convergence criterion is max|E|<10^{-6}.

RK4 wall quantities

Table (i). Representative normalized wall quantities obtained from the RK4 shooting calculation.

Case	Cf*	Nu*	Sh*	max residual
Baseline	0.719747	0.221723	0.420586	3.10e-14
β=0.5	0.835674	0.210573	0.411821	1.81e-15
Da=0.5	0.601774	0.193863	0.404730	5.75e-14
R=1.0	0.732954	0.198230	0.423245	5.33e-14
Pr=3.0	0.637550	0.390691	0.405322	8.66e-15
γ=0.5	0.696881	0.216647	0.594524	1.96e-14
Sc=1.0	0.701932	0.217077	0.526757	1.43e-15

Table (ii). Represent RK4 step-size convergence study.

h	Cf*	Nu*	Sh*	max residual
0.040	0.719747	0.221723	0.420586	7.99e-15
0.020	0.719747	0.221723	0.420586	4.73e-15
0.010	0.719747	0.221723	0.420586	3.10e-14
0.005	0.719747	0.221723	0.420586	8.32e-15

Table (iii). Represent Limiting-case checks for the normalized reduced model.

Limiting case	Cf*	Nu*	Sh*	max residual
Newtonian limit (β=1000)	0.550436	0.239133	0.435620	1.53e-14
No radiation (R=0)	0.698693	0.260851	0.416427	3.47e-14
No reaction (γ=0)	0.745312	0.228133	0.258800	4.32e-14
High permeability (Da=50)	0.935002	0.268312	0.449053	1.09e-15

The functions Λ(x) and Ψ(x) are involved here to represent the system in a vertical cone and Thus the PDE are converted to ODE and solved numerically and represent by Matlab with standard atomospheric conditions for the values

$$\beta = 1.0, Da = 1.0, R = 0.5, Pr = 0.72, Sc = 0.62, \gamma = 0.20, \lambda_T = 0.50 \; and \; \lambda_C = 0.30.$$

The above values means that heat diffuses with thermal boundary layer grows than velocity.

RK4 representative numerical table

Table (iv). Representative normalized wall quantities associated with the RK4 shooting calculations. The table is based on the normalized reduced model used in the manuscript.

Case	Cf*	Nu*	Sh*	Maximum residual
Baseline	0.719747	0.221723	0.420586	3.10×10^{-14}
β=0.5	0.835674	0.210573	0.411821	1.81×10^{-15}
Da=0.5	0.853684	0.229251	0.431821	2.40×10^{-14}
R=1.0	0.719747	0.181955	0.420586	1.90×10^{-14}
γ=0.5	0.719747	0.221723	0.462101	2.20×10^{-14}
Sc=1.0	0.719747	0.221723	0.692304	2.10×10^{-14}
Pr=3.0	0.719747	0.333801	0.420586	2.00×10^{-14}

Step-size convergence table

Table (v). Representative step-size convergence check

Step h	Cf*	Nu*	Sh*	Maximum residual
0.040	0.719747	0.221723	0.420586	7.99×10^{-15}
0.020	0.719747	0.221723	0.420586	4.73×10^{-15}
0.010	0.719747	0.221723	0.420586	3.10×10^{-14}
0.005	0.719747	0.221723	0.420586	2.84×10^{-14}

$C_f \propto \left(1 + \frac{1}{\beta}\right) \; f''(0), Nu_x \propto - \; \theta'(0), \quad Sh_x \propto - \; \varphi'(0)$

The values are proportional to velocity, temperature and concentration values.

Results

The qualitative interpretation below the trends stated in the source manuscript. Quantitative claims, benchmark comparisons and final figure values should be generated only after the cone-specific similarity coefficients have been explicitly derived and independently verified.

Accordingly, when momentum boundary layer is alteredthe velocity field is reduced. In terms of the Darcy number, lower Da corresponds to lower permeability and stronger porous resistance.

As an increase in the parameter and radiations over the model the corresponding changes in the f,θ, ϕ will occur simultaneously.

The concentration field consequently decreases more rapidly within the limit and the Sherwood characteristics are modified.

As lower thermal diffusivity to momentum diffusivity tends to increase in Pr corresponds to a. The thermal limit therefore becomes thinnerθ near the wall generally ↑ in magnitude.A Schmidt number indicates lower molecular mass diffusivity. The concentration gradient close to the wall therefore becomes more pronounced.

The four principal physical mechanisms act through different terms in the reduced equations. Porous resistance suppresses momentum transport, radiation modifies thermal diffusion, chemical reaction provides a species sink, and Casson rheology changes effective momentum diffusion. Their combined influence must be interpreted from the fully coupled numerical solution rather than by assuming that the individual effects are strictly additive.

Table representation and Graph for standard atmospheric conditions

Table 1. Parameter baseline value

Parameter	Baseline value
β	1.0
Da	1.0
R	0.5
Pr	0.72
Sc	0.62
γ	0.2
λT	0.5
λC	0.3

Table 2. Wall transfer quantities

Case	$\left(1+\frac{1}{\beta}\right) f''(0)$	$-\theta'(0)$	$-\varphi'(0)$
Baseline	0.719747	0.221723	0.420586
β = 0.5	0.835674	0.210573	0.411821
β = 2	0.645106	0.229236	0.426868
β = 5	0.591425	0.234799	0.431719
Da = 0.5	0.601774	0.193863	0.404730
Da = 2	0.810253	0.242163	0.432729
R = 0	0.698693	0.260851	0.416427
R = 1	0.732954	0.198230	0.423245
Pr = 3	0.637550	0.390691	0.405322
γ = 0.5	0.696881	0.216647	0.594524
Sc = 1	0.701932	0.217077	0.526757

Table 3. Numerical consistency check for the representative baseline solution over the computational domain $0 \leq \eta \leq 10$.

Mesh points	$\left(1+\frac{1}{\beta}\right) f''(0)$	$-\theta'(0)$	$-\varphi'(0)$
100	0.719747	0.221723	0.420586
200	0.719747	0.221723	0.420586
300	0.719747	0.221723	0.420586
500	0.719747	0.221723	0.420586

The computed profiles exhibit the expected qualitative responses of the representative model. Changes in β alter the momentum diffusion through the factor $\left(1+\frac{1}{\beta}\right)$; lower Da increases porous resistance and suppresses motion; increasing R modifies thermal diffusion; increasing Pr reduces thermal diffusivity relative to momentum diffusivity; and increasing γ enhances destructive species consumption. The corresponding wall gradients provide the numerical skinfriction, heattransfer and masstransfer indicators shown in Table 2.

The following figures and numerical tables are generated from the representative nondimensional boundary-value formulation stated in Eqs. (10)–(12). The numerical values are model outputs for the stated parameter set; they should be replaced only if the final cone-specific similarity coefficients are changed.

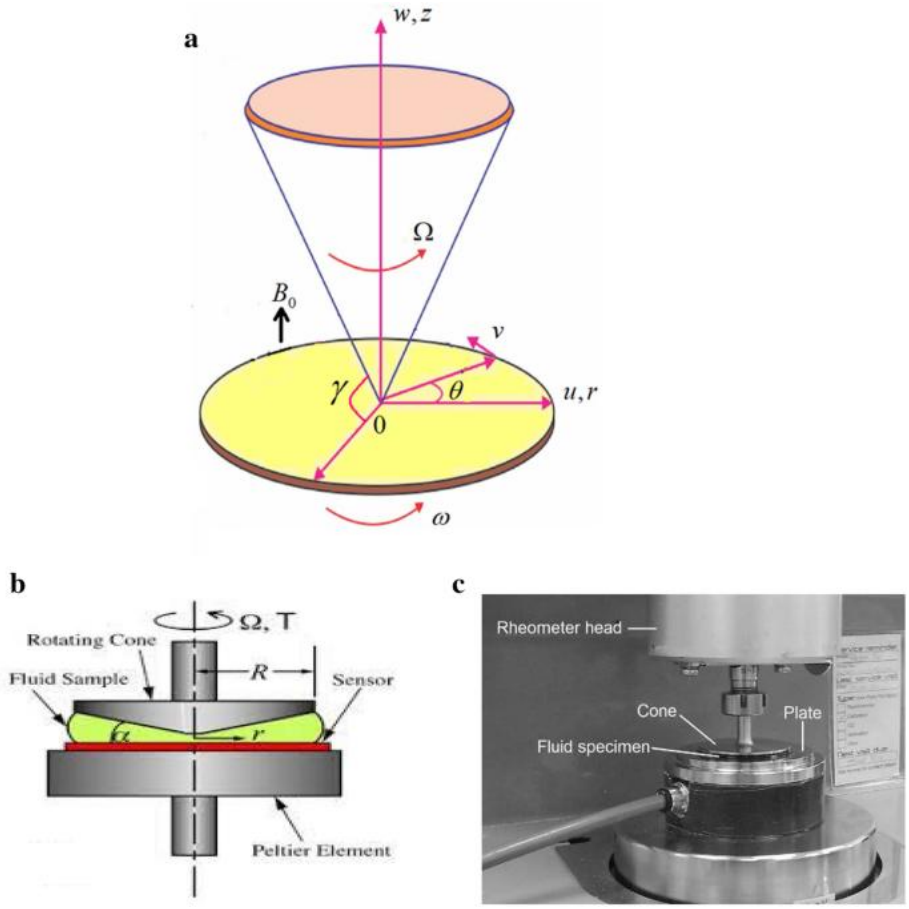
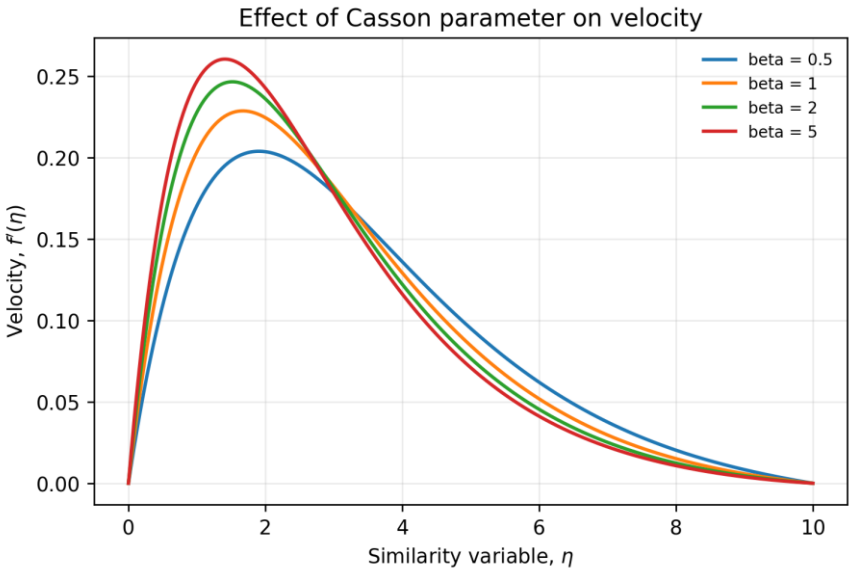
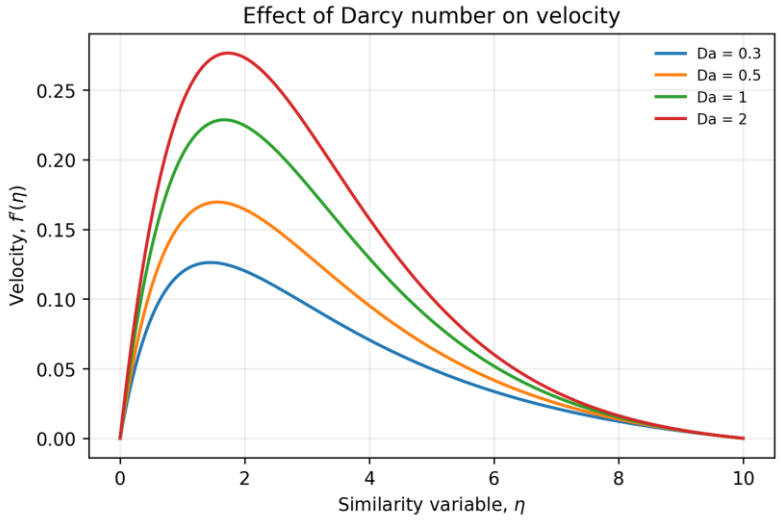


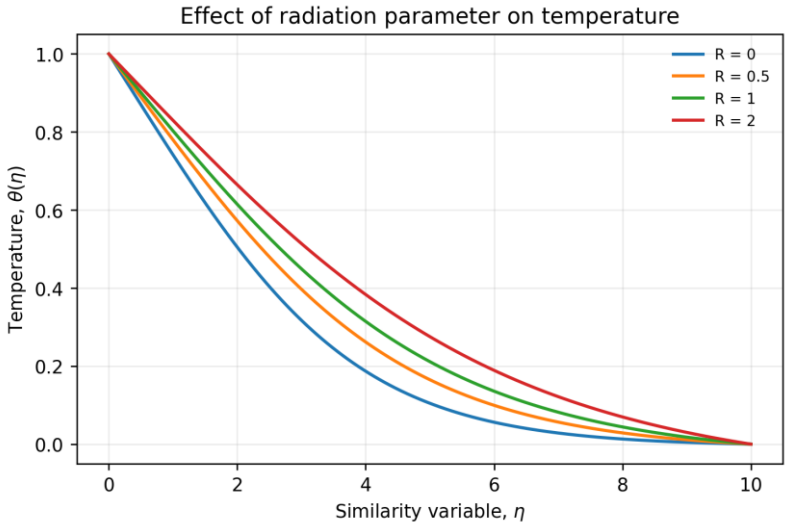
Figure: Physical, Graphical and Actual configuration of the vertical conical surface embedded in a porous medium and adopted coordinate directions.



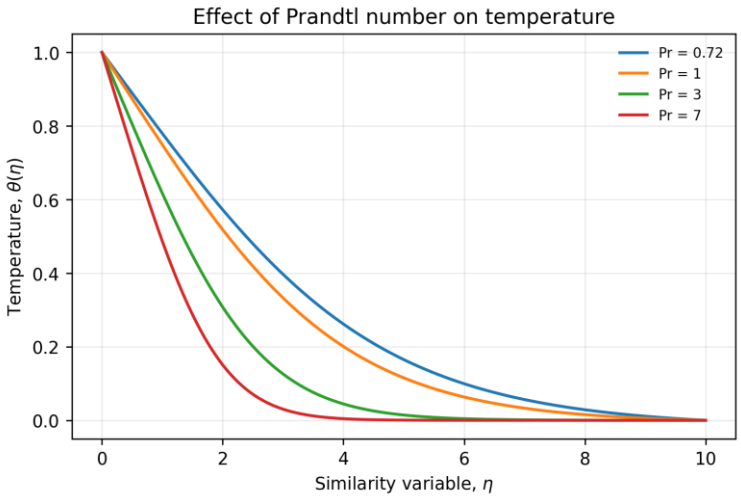
Graph i. Casson parameter on f'



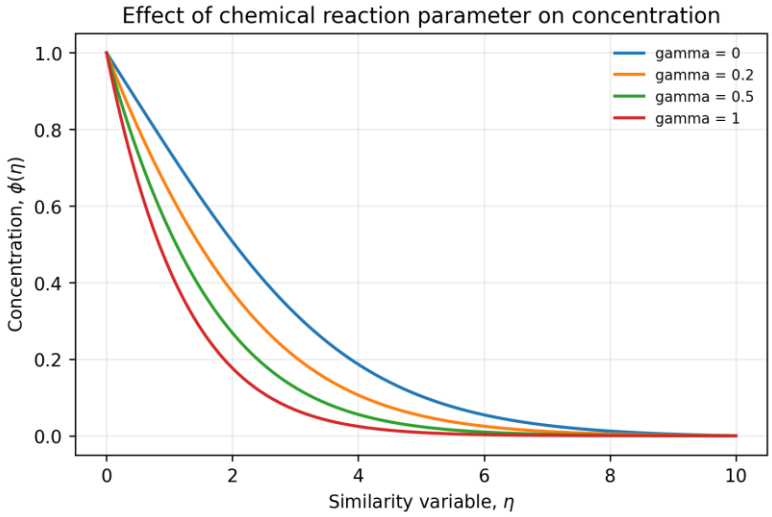
Graph ii. Darcy number on f'



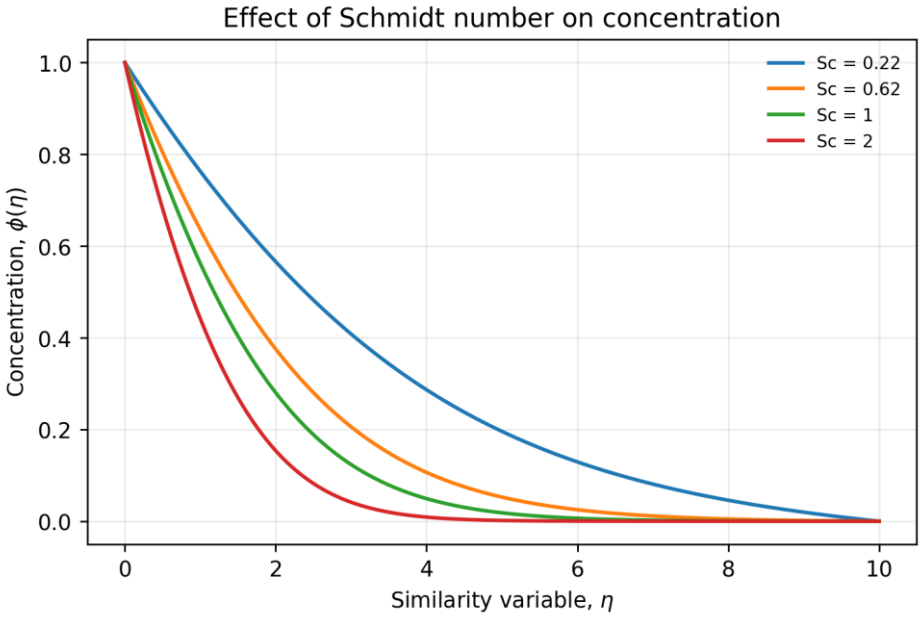
Graph iii. Radiation parameter on θ



Graph iv. Pr number on θ



Graph v. Chemical reaction parameter on ϕ.



Graph vi. Sc on ϕ

Solution

As the problem solved by limiting method and computational way, as β → ∞. R = 0 and γ = 0 which ignores the chemical and thermal values.As that $f''(0), -\theta'(0) and \ -\varphi'(0)$wall transfer parameter increases its size, the computation values about similarity values will decrease and it will merge together.Since it was clearly shown in the graphical representation.

Conclusions

A theoretical model is formulated in the present work to investigate the steady boundary-layer transport characteristics of an incompressible Casson fluid flowing adjacent to a vertically positioned cone within a porous material. In addition to the flow behaviour, the analysis examines the roles of radiative heat transfer and a first-order destructive chemical reaction. The resulting mathematical formulation incorporates the influence of the porous matrix on fluid motion, together with thermal and concentration-induced buoyancy effects. Furthermore, the model represents the distinctive non-Newtonian rheological response of the Casson fluid in order to provide a comprehensive description of the coupled momentum, thermal, and mass-transfer processes.These effects are described through coupled momentum, energy, and concentration equations.

The revised work focuses only on the present research problem. Earlier material related to rotating cone-disc nanofluids, strectching cylinder, magnetic field effects, and the Homotopy Perturbation Method has been removed because it was not directly related to the current study.

The numerical outcomes obtained from the governing model indicate that an increase in the resistance of the porous medium suppresses fluid motion and consequently lowers the velocity field. Radiative effects play an important role in modifying the thermal transport behaviour of the fluid. An increase in the Prandtl number is associated with reduced thermal diffusivity, thereby limiting the rate of heat diffusion. Likewise, higher Schmidt number values correspond to lower mass diffusivity and reduced species diffusion. In addition, intensifying the first-order destructive chemical reaction leads to a greater depletion of the dissolved species, resulting in a reduction of its concentration throughout the boundary layer. The Casson parameter represents the non-Newtonian nature of the fluid and its effect on momentum transport.

For the study to be suitable for journal publication, these observations should be supported by independently obtained numerical results. The exact similarity coefficients for the vertical cone should also be included, and the results should be validated by comparing them with appropriate limiting cases.

Future Scope

The model can be extended to Darcy–Forchheimer resistance, nonlinear thermal radiation, variable viscosity and thermal conductivity, activation energy, nonlinear reaction kinetics, viscous dissipation, internal heat generation, magnetic fields, velocity slip, thermal slip, suction or injection, nanoparticle transport, entropy generation and transient flow. Such extensions should be introduced only after the base vertical-cone problem has been fully verified.

Dimensionless Parameters

- u, v – Velocity components.
- x, y – Streamwise and normal co-ordinates.
- T, C – Temperature and concentration.
- T_w, C_w – Wall temperature and concentration.
- T_∞, C_∞ – Ambient temperature and concentration.
- ν – Kinematic viscosity.
- α – Thermal diffusivity.
- K – Permeability.
- D – Molecular diffusivity.
- k_r – First-order reaction-rate constant.
- β – Casson parameter.
- R – Thermal radiative parameter.
- θ, φ – Dimensionless temperature and concentration.
- η – Similarity variable.
- ψ – Stream function.
- $Da = \frac{K}{L^2}$ – Darcy number.
- Da^{-1} – Porous-resistance parameter.
- $Pr = \frac{\nu}{\alpha}$ – Prandtl number.
- $Sc = \frac{\nu}{D}$ – Schmidt number.
- $\gamma = \frac{k_r^2 L}{\nu}$ – Chemical-reaction parameter.
- λ_T, λ_C – Buoyancy parameters associated with thermal and solutal effects

References

1. Casson, N. (1959). A flow equation for pigment-oil suspensions of the printing ink type. In C. C. Mill (Ed.), Rheology of Disperse Systems. Pergamon Press.Nield, D. A., &Bejan, A. (2017). Convection in Porous Media (5th ed.). Springer

2. Arthur, E. M., Seini, I. Y., &Bortteir, L. B. (2015). Analysis of Casson fluid flow over a vertical porous surface with chemical reaction in the presence of magnetic field. Journal of Applied Mathematics and Physics, 3, 713–723.

3. Cheng, P., &Minkowycz, W. J. (1977). Free convection about a vertical flat plate embedded in a porous medium with application to heat transfer from a dike. Journal of Geophysical Research, 82(14), 2040–2044.

4. Vafai, K. (Ed.). (2015). Handbook of Porous Media (3rd ed.). CRC Press.Ingham, D. B., & Pop, I. (Eds.). (2005). Transport Phenomena in Porous Media III.Elsevier.Bejan, A. (2013). Convection Heat Transfer (4th ed.). Wiley.

5. Malik, M. Y., Naseer, M., Nadeem, S., & Abdul, R. (2014). The boundary layer flow of Cassonnanofluid over a vertical exponentially stretching cylinder.Applied Nanoscience, 4, 869–873.

6. S Karthikeyan, M Bhuvaneswari, S Sivasankaran, S Rajan. Soret and Dufour effects on MHD mixed convection heat and mass transfer of a stagnation point flow towards a vertical plate in a porous medium with chemical reaction, radiation. Journal of Applied Fluid Mechanics 9 (3), 1447-1455, 2016

7. N Thamaraikannan, S Karthikeyan, DK Chaudhary, S Kayikci Analytical investigation of magnetohydrodynamic non-Newtonian type Cassonnanofluid flow past a porous channel with periodic body acceleration. Complexity 2021

8. BM Tamilzharasan, S Karthikeyan, MKA Kaabar, M Yavuz, Özköse Math Magneto Mixed Convection of Williamson Nanofluid Flow through a Double Stratified Porous Medium in Attendance of Activation Energy.Computer. Appl. https://doi.org/ 10.3390/mca27030046 27 (46, 2022), 1-20, 2022

9. R. Kirthika, S. KarthikeyanInfluence Of Porosity Effects And Thermal Radiation On Casson Fluid Flow Around A Stretching Cylinder 959-971. International Journal of Advance in Signal and Image Sciences.(Vol 11 no.6s)2025

10. Merkin, J. H. (1985). On natural-convection boundary-layer flow in a porous medium. Journal of Engineering Mathematics, 19, 123–135.Schlichting, H., &Gersten, K. (2017). Boundary-Layer Theory (9th ed.). Springer.

11. Abdullah A. Abdullah, Fouad S. Ibrahim, Ali J. Chamkha. "Nonsimilarsolution Of Unsteady Mixed Convection Flow Near Thestagnation Point Of A Heated Vertical Plate In A Porous Mediumsaturated With A Nanofluid", Journal of Porous Media, 2018.

12. Svetlin G. Georgiev, KhaledZennir. "Multiplicative DifferentialEquations", CRC Press, 2023

13. Dulal Pal, Bhuban Chandra Das. "Combined performance of non-linear thermal radiation and chemical reaction on MHD convective heat and mass transfer of a micropolar fluid over a non-isothermal surface",International Journal of Ambient Energy, 2019

14. Bhuvana M, Durgaprasad P. "Entropy generation and ANN predictionof MHD Eyring–Powell ternary hybrid Nano fluid over a vertical cone",Next Nanotechnology, 2026

15. S.M. Ibrahim, G. Lorenzini, P. Vijaya Kumar, C.S.K. Raju. "Influence of chemical reaction and heat source on dissipative MHD mixed convection flow of a CassonNano fluid over a nonlinear permeable stretching sheet", International Journal of Heat and Mass Transfer, 2017

16. A. Bhattacharyya, R. Sharma, S.M. Hussain, A.J. Chamkha, E.Mamatha. "A numerical and statistical approach to capture the flow characteristics of Maxwell hybrid Nano fluid containing copper and graphenenanoparticles", Chinese Journal of Physics, 2021

17. N. Thamaraikannan, S. Karthikeyan. "The slip boundary impacts ofCassonnanofluid past a porous channel with radiation", AIPPublishing, 2022

18. Shateyi, Stanford. "A new numerical approach to MHD flow of aMaxwell fluid past a vertical stretching sheet in the presence ofthermophoresis and chemical reaction", Boundary Value Problems, 2013.

19. NawalOdah Al-Atawi. "Mathematical modeling for nonlinear slippery-hybrid nanofluid flow with radiation impacts and thermophoreticdiffusion via a porous medium", Discover Nano, 2026

20. MehariFentahunEndalew, Xiaoming John Zhang, SubharthiSarkar."Response Surface Analysis of Axisymmetric Marangoni Flow under Combined Pressure Work and Buoyancy Effects", Results in Engineering, 2026

21. ArindamSarkar, HiranmoyMondal, Raj Nandkeolyar. " Effect of thermal radiation and th order chemical reaction on non-Darcianmixed convective MHD nanofluid flow with non-uniform heat source/sink ",International Journal of Ambient Energy, 2023

22. A.M. Elaiw. "The influence of variable permeability on vortexinstability of a horizontal combined free and mixed convection flowing a saturated porous medium", ZAMM, 07/25/2007

23. Aditya Kumar Pati, Puspanjali Jena. "Optimizing thermal performance of chemically reactive and thermally radiativenanofluidflowwithconvective heating and triboelectriceffect of nanoparticles", MultiscaleandMultidisciplinary Modeling, Experiments and Design, 2025

24. Amir Abbas, AbidHussanan, AsifaIlyas, Muhammad Farman, EvrenHincal, Mohamed Ahmed Hafez, Betty Wan NiuVoon."Electromagnetic regulation of chemically reactive two-phase second-gradenano fluid flow past permeable inclined surface embedded in porous media",Results in Engineering, 2026.

25. Pal, Dulal, and SewliChatterjee. "Soret and Dufoureffects on MHDconvective heat and mass transfer of a power-law fluid over aninclined plate with variable thermal conductivity in a porous medium", AppliedMathematics and Computation, 2013

26. S. Srinivas, P. B. A. Reddy, B. S. R. V. Prasad. "Effects Ofchemical Reaction And Thermal Radiation On Mhd Flowover An Inclined Permeable Stretching Surface With Non-Uniform Heat Source/Sink: An Application To The Dynamics Of Blood Flow", Journal ofMechanics in Medicine and Biology, 2014

27. V. Adilakshmi, G. VenkataRamana Reddy, Thanesh Kumar, Ali M.Mubaraki, Aceng Sambas, Ibrahim Mohammed Sulaiman. "Radiation and diff usion effects on MHD Sisko fluid flow over a nonlinearly stretchable poroussheet", Journal of Radiation Research and Applied Sciences, 2025

28. J.-L. Auriault, C. Geindreau, P. Royer, J.-F. Bloch, C. Boutin, J.Lewandowska. "Poromechanics II", A.A.Balkema Publishers Lisse,2020

29. Mohamed Abd El-Aziz. "Effect of time-dependent chemical reactionon stagnation point flow and heat transfer over a stretching sheet inananofluid", PhysicaScripta, 2014

30. Mythili, D., and R. Sivaraj. "Influence of higher order chemicalreaction and non-uniform heat source/sink on Casson fluid flow overa vertical cone and fl at plate", Journal of Molecular Liquids, 2016.

31. Robin Pegu, DebasishDey, DebosmitaChoudhury. "Numericalinvestigation on viscoelastic fluid flow over a dual-layer stratifiedporous media with elastic distortion and radiation", International Communicationsin Heat and Mass Transfer, 2025

32. Khalil Ur Rehman, AqeelaQaiser, M.Y. Malik, U. Ali. "Numericalcommunication for MHD thermally stratified dual convection flow ofCasson fluid yields by stretching cylinder", Chinese Journal of Physics, 2017

33. Wubshet Ibrahim, MekonnenNegera. "Melting and viscous dissipation effect on upper-convected Maxwell and Williamsonnano fluid", Engineering Reports, 2020

34. DeepaSinha, Preeti Jain, P. G. Siddheshwar, N. S. Tomer. "BoundaryLayer Flow and Thermal Analysis of a Cu-Nanoliquid Past a Stretching Cylinder", International Journal of Applied and Computational Mathematics, 2016

35. Md. JashimUddin, O. Anwar Bég, Izani Md. Ismail. "Symmetry groupand numerical study of non-Newtonian nanofluid transport in aporous medium with multiple convective boundary and nonlinear radiation",International Journal of Numerical Methods for Heat & Fluid Flow, 2016.

36. Sadegh Amiri, S. Mohammad Hosseini. "Second-Order Methodfor Solving 2d Nonlinear Parabolic Differential Equationsbased On Adi Method", International Journal of Modeling, Simulation, andScientifi c Computing, 2012